An experimental study on elastic electron-trifluoromethane (CHF₃) scattering in the low and intermediate energy ranges

I Iga[1]**, P Rawat**[1]**, I P Sanches**[1]**, M-T Lee**[1]** and M G P Homem**[2,3]

[1] Departamento de Química, UFSCar, 13565-905 São Carlos, SP, Brazil
[2] Laboratório Nacional de Luz Síncrotron-LNLS, 13083-970 Campinas, SP, Brazil
[3] Departamento de Física, UFSCar, 13565-905 São Carlos, SP, Brazil

Abstract
In this work, we report an experimental study on elastic electron collisions with CHF₃ in the low and intermediate energy range. More specifically, absolute differential, integral and momentum transfer cross sections are measured and reported in the 20–500 eV range. The measurements were performed using a crossed electron beam–molecular beam geometry. The angular distributions of the scattered electrons were converted to absolute cross sections using the relative flow technique. Integral and momentum transfer cross sections are derived from the measured differential cross sections. A comparison between our measured data with the theoretical and other experimental results available in the literature is made.

1. Introduction

Electron scattering from polyatomic molecules composed of carbon, hydrogen and halogen atoms is a subject of an increasing interest, both theoretically and experimentally due to the role played by these compounds in various fields of application. In particular, trifluoromethane (CHF₃) can be used as an etchant gas in the manufacture of semiconductors [1]. Discharge decomposition of this molecule gives rise to fluorine and various neutral radicals, which play a fundamental role for etching SiO_2 and for polymer growth on Si, enhancing the etch selectivity of SiO_2 and Si [2]. Therefore, data of electron impact cross sections for CHF₃ are needed to understand and model the fluorine-based plasma etching system [3]. They are also important to elucidate some mechanisms and/or to control plasma processing in industry [4].

During the past 10 years, there have been many experimental investigations on electron–CHF₃ scattering reported in the literature. Some experimental investigations on this matter were summarized in two review articles [5, 6]. Elastic electron differential cross sections (DCS) were first reported by Tanaka *et al* [7] at three incident energies namely, 1.5, 30 and 100 eV, and more recently by Varella *et al* [8] in the 2–30 eV range. Also, momentum

transfer cross sections (MTCS) up to 200 eV were generated by Kushner and Zhang [9] from experimental swarm parameters. In 1998, grand total cross sections (TCS) were measured by Sueoka *et al* [10] in the 0.7–600 eV energy range and by Sanabia *et al* [11] in the 0.1–20 eV range. More recently, TCS for this target were also measured by Nishimura and Nakamura [12] and by Iga *et al* [13]. Threshold electron impact ionization of trifluoromethane was investigated by Fiegele *et al* [14]. Experimental cross sections for electron impact dissociation into neutral and ionic radicals were presented by Goto *et al* [2]. Electron impact partial and total ionization cross sections (TICS) were reported by Poll and Meischner [15], Goto *et al* [2] and Jiao *et al* [16], and more recently by Iga *et al* [17] and by Torres *et al* [18]. Moreover, ion–photon coincidence of CHF_3 by controlled electron impact was investigated by Furuya *et al* [19].

On the theoretical side, several investigations on e^-–CHF_3 scattering have also appeared in the literature during the past decade. Natalense *et al* [20] calculated DCS, integral cross sections (ICS) and MTCS for this molecule using the Schwinger multichannel method (SMC) with norm-conserved pseudopotentials. Also using the SMC but with Born-closure procedure, DCS, ICS and MTCS for elastic electron collision on this target were reported by Varella *et al* [8] in the 2–30 eV range. More recently, elastic and excitation cross sections for electron–CHF_3 scattering in the 0–50 eV were calculated and reported by Morgan *et al* [21]. Finally, DCS and ICS in the 0.1–10 000 eV range were calculated by Manero *et al* [22] using the independent atom model (IAM).

Despite the intense theoretical and experimental activities on e^-–CHF_3 scattering studies in the past years, not much was done regarding experimental investigation on elastic e^-–CHF_3 scatterings. DCS for this target have been measured by only one group [7, 8] and limited for incident energies equal to and below 100 eV. Above that energy, there is a lack of both theoretical and experimental data for elastic e^-–CHF_3 collisions. Considering the importance of this molecule in various fields of application, more experimental determination of such cross sections would be interesting, not only to confirm the existing results but also to produce new data, particularly extensive to higher incident energies. Also from the fundamental point of view, the results at higher incident energies will be useful for the test of the reliability of the IAM in the intermediate energy range. In this paper, we report an experimental investigation on elastic electron scattering by CHF_3. Absolute DCS determined using the relative flow technique (RFT) [23–25] in the 20–500 eV range are reported. ICS and MTCS in this range are also derived from the DCS, measured in the $10°$–$130°$ angular range and extrapolated to forward and backward directions. In addition, an estimate of TCS is made by adding the present ICS with the TICS of Iga *et al* [17]. Comparison of the estimated and the experimental TCS [10, 12, 13] may provide an estimate of the importance of other inelastic channels (excitation and dissociation) but ionization. This comparison can also provide a test of the reliability of the present experimental data at the higher end of incident energies.

The organization of this paper is as follows. In section 2, some experimental details are briefly presented. Finally, in section 3 our experimental results are compared with existing theoretical and/or experimental data.

2. Experimental details

Details of our experimental set-up and procedure have already been presented in our previous works [26, 27] and will only be briefly outlined here. A crossed electron beam–molecular beam geometry is used to measure the relative distribution of the scattered electrons as a function of the scattering angle at a given incident electron energy. The scattered electrons are energy-filtered by a retarding-field energy selector with a resolution of about 1.5 eV. With this resolution, it is sufficient to distinguish inelastically scattered electrons resulting from

Table 1. Experimental DCS, ICS and MTCS (in 10^{-16} cm^2) for elastic e$^-$–CHF$_3$ scattering.

Angle (degree)	E_0 (eV)			
	20	30	50	75
10	2.22(1)	2.45(1)	2.25(1)[a]	1.73(1)
15	9.79(0)	1.48(1)	1.27(1)	8.40(0)
20	6.36(0)	9.25(0)	6.14(0)	3.70(0)
25	5.03(0)	5.85(0)		
30	3.77(0)	3.09(0)	1.53(0)	7.55(−1)
35	2.63(0)	2.03(0)		
40	1.69(0)	1.15(0)	6.76(−1)	5.39(−1)
45	1.22(0)	8.85(−1)		
50	8.35(−1)	7.26(−1)	6.29(−1)	2.90(−1)
55	7.63(−1)	7.64(−1)		
60	7.36(−1)	7.63(−1)	4.38(−1)	1.55(−1)
65	7.91(−1)	7.30(−1)		
70	8.08(−1)	6.57(−1)	2.38(−1)	1.04(−1)
75	7.36(−1)	5.64(−1)		
80	6.46(−1)	4.36(−1)	1.44(−1)	8.10(−2)
85	6.56(−1)	3.31(−1)		
90	6.29(−1)	2.51(−1)	1.08(−1)	6.90(−2)
95	5.48(−1)	2.23(−1)		
100	5.48(−1)	2.23(−1)	1.02(−1)	6.82(−2)
105	4.85(−1)	2.56(−1)		
110	4.58(−1)	2.72(−1)	1.45(−1)	8.74(−2)
115	5.12(−1)	3.39(−1)		
120	5.39(−1)	4.28(−1)	2.92(−1)	1.40(−1)
125	5.30(−1)	6.20(−1)		
130			4.48(−1)	2.22(−1)
ICS	2.00(1)	1.92(1)	1.31(1)	1.23(1)
MTCS	1.03(1)	1.00(1)	5.27(0)	2.74(0)

electronic excitation for the molecule under study since the lowest excitation threshold of CHF$_3$ is 4.95 eV [5]. Nevertheless, it is unable to separate those from vibrational excitation processes. Therefore, our measured DCS are indeed vibrationally summed. During the measurements, the working pressure in the vacuum chamber is around 5×10^{-7} Torr. The recorded scattering intensities are converted into absolute elastic DCS using the RFT [23–25]. Accordingly, the DCS for a gas under determination (x) can be related with the known DCS of a secondary standard (std) as

$$(\text{DCS})_x = (\text{DCS})_{\text{std}} \frac{I_x}{I_{\text{std}}} \frac{n_{\text{std}}}{n_x} \left(\frac{M_{\text{std}}}{M_x} \right)^{\frac{1}{2}}, \tag{1}$$

where, I is the scattered electron intensity, n is the flow rate and M is the molecular weight. The above equation is valid if the beam profiles (density distribution) of both gases, x and std, are nearly the same. According to Olander and Kruger [28], this requirement is fulfilled under two conditions: the equal mean free paths (λ) of the gases behind the capillaries and the Knudsen number K_L defined as $\frac{\lambda}{L}$ varying between $\gamma \leqslant K_L \leqslant 10$, where $\gamma = d/L$ is the aspect ratio of an individual capillary with diameter d and length L. However, several recent investigations have provided experimental evidence that even at beam flow regimes in which the K_L are significantly lower than γ, the above relationship can still be valid [25, 26].

Table 1. (Continued.)

Angle (deg)	E_0 (eV)					
	100	150	200	300	400	500
10	2.41(1)	2.02(1)	1.31(1)	8.39(0)	4.07(0)	4.24(0)
15	9.61(0)	6.81(0)	2.84(0)	2.32(0)	1.84(0)	1.80(0)
20	3.14(0)	2.32(0)	1.52(0)	1.59(0)	1.39(0)	6.79(−1)
25	1.40(0)	1.50(0)	1.23(0)	1.19(0)	8.60(−1)	
30	1.05(0)	1.19(0)	8.34(−1)	6.97(−1)	6.17(−1)	5.45(−1)
35	8.18(−1)	7.84(−1)	5.08(−1)	5.69(−1)	4.67(−1)	
40	5.90(−1)	4.93(−1)	3.81(−1)	4.40(−1)	2.68(−1)	1.55(−1)
45	3.81(−1)	3.52(−1)	3.31(−1)	2.96(−1)	1.65(−1)	
50	2.71(−1)	2.98(−1)	2.73(−1)	1.90(−1)	1.36(−1)	1.12(−1)
55	2.14(−1)	2.48(−1)	2.03(−1)	1.46(−1)	1.27(−1)	
60	1.76(−1)	1.97(−1)	1.42(−1)	1.33(−1)	1.05(−1)	6.47(−2)
65	1.70(−1)	1.30(−1)	1.03(−1)	1.28(−1)	8.90(−2)	
70	1.34(−1)	9.70(−2)	9.60(−2)	1.13(−1)	7.60(−2)	4.10(−2)
75	1.11(−1)	7.70(−2)	9.20(−2)	1.05(−1)	6.60(−2)	
80	7.90(−2)	7.00(−2)	9.50(−2)	1.01(−1)	5.60(−2)	3.46(−2)
85	6.40(−2)	6.80(−2)	9.20(−2)	9.80(−2)	5.40(−2)	
90	5.60(−2)	7.20(−2)	8.80(−2)	8.60(−2)	5.10(−2)	2.63(−2)
95	5.50(−2)	7.50(−2)	8.90(−2)	7.90(−2)	4.90(−2)	
100	5.30(−2)	7.60(−2)	9.00(−2)	7.80(−2)	4.40(−2)	2.36(−2)
105	6.30(−2)	7.80(−2)	8.50(−2)	7.40(−2)	4.00(−2)	
110	8.70(−2)	8.80(−2)	8.60(−3)	7.30(−3)	4.00(−2)	1.99(−2)
115	1.05(−1)	9.50(−2)	9.00(−2)	6.70(−2)	3.80(−2)	
120	1.28(−1)	1.02(−1)	9.00(−2)	6.70(−2)	3.70(−2)	1.70(−2)
125	1.61(−1)	1.15(−1)	9.80(−2)	6.90(−2)	3.80(−2)	
130	1.84(−1)	1.26(−1)	9.90(−2)	7.20(−2)	3.60(−2)	1.74(−2)
135	2.19(−1)	1.36(−1)	1.00(−1)	7.40(−2)	3.70(−2)	
ICS	1.06(1)	8.36(0)	6.93(0)	5.22(0)	4.11(0)	3.29(0)
MTCS	2.47(0)	1.77(0)	1.44(0)	1.23(0)	7.40(−1)	4.20(−1)

[a] 2.25(1) means 2.25×10^1.

In principle, all gaseous targets could be chosen as a secondary standard. The only requirement is that reliable DCS covering the energy and angular ranges of interest are available in the literature for elastic electron scattering from the chosen target. In practice, the existence of a highly reliable DCS set for elastic e^-–He scattering in the low energy range [29] makes this gas widely used as a secondary standard in the experimental DCS determinations. In 1993, Buckman *et al* [30] investigated the spatial profiles of effusive molecular beams for several gases. They found that the full-width at half-maximum (FWHM) of the beam profiles were very similar for species Ar, Ne, N_2 and Kr in a wide range of λ (from 0.005 mm to 5 mm). On the other hand, the FWHM of He and H_2 beams are significantly smaller than those of heavier species at $\lambda \leqslant 0.1$ mm region. Based on the above observation, it can then be expected that the use of a secondary standard heavier than He would allow us to obtain accurate DCS for most of the species, in a more extensive region of λ.

In the present study, Ar is used as the secondary standard. Absolute DCS of Jansen *et al* [31] in the 100–500 eV energy range and those of Panajotović *et al* [32] in the 20–75 eV are used to normalize our data. Details of the analysis of experimental uncertainties have also been given elsewhere [26]. They are estimated briefly as follows. Uncertainties of random nature such as pressure fluctuations, electron beam current readings, background scattering,
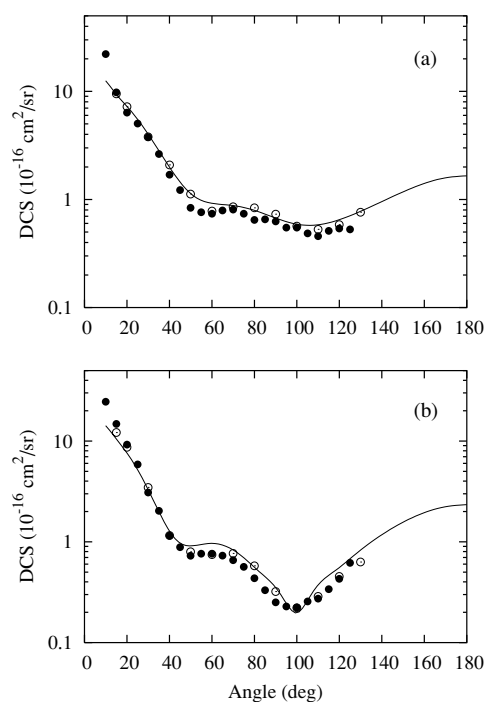
Figure 1. DCS for e$^-$–CHF$_3$ scattering at incident energies of (a) 20 eV and (b) 30 eV. Full circles, present experimental results; open circles, experimental results of Varella *et al* [8]; solid line, calculated results of Varella *et al* [8].

etc, are estimated to be less than 2%. These contributions combined with the estimated statistical errors give an overall uncertainty of 4% in the relative DCS for each gas. Also, the experimental uncertainty associated with the normalization procedure is estimated to be 5.7%. These errors combined with the quoted errors [31, 32] in the absolute DCS of the secondary standard provide overall experimental uncertainties of 11% in the (100–500) eV range and 23% elsewhere in our absolute DCS. The absolute DCS were determined in the 10°–135° angular range. In order to obtain ICS and MTCS, an extrapolation procedure was adopted to estimate DCS at scattering angles out of that range. The extrapolation was carried out manually. The overall errors on ICS and MTCS are estimated to be 22% in the (100–500) eV range and 30% below 100 eV.

3. Results and discussion

The present experimental data of DCS, ICS and MTCS, obtained in the 20–500 eV energy range, are presented in table 1. Some representative results of DCS at selected incident energies, mostly when other experimental and/or calculated data are available, are also plotted. In figures 1 and 2, we present our experimental DCS in the 20–200 eV energy range. The experimental and theoretical results of Varella *et al* [8] at 20 and 30 eV, the experimental DCS of Tanaka *et al* [7] at 100 eV, and the calculated results of Manero *et al* [22] using the IAM at 100 and 200 eV are also shown for comparison. It is seen that there is a very good agreement, both qualitatively and quantitatively, between our measured DCS at 20 and 30 eV and experimental and calculated data of Varella *et al* [8]. Also, at 100 eV, our measured
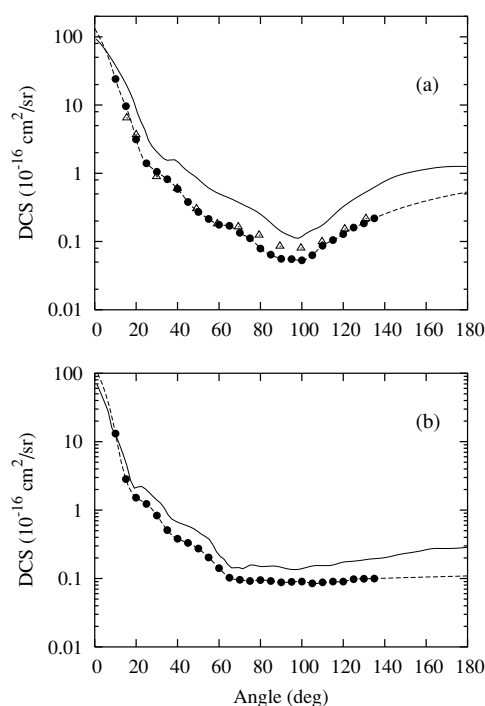
Figure 2. The same as figure 1, but for (a) 100 eV and (b) 200 eV. The symbols are the same as in figure 2, except open triangles, measured DCS of Tanaka *et al* [7]; solid line, the IAM data of Manero *et al* [22]; short-dashed line, present interpolated–extrapolated data.

data agree well with those reported by Tanaka *et al* [7]. This fact itself is very interesting since the measurements were performed independently by our group and by the group of Tanaka *et al* with different energy analysers and different secondary standards. Therefore, this good agreement may reflect the reliability of the DCS of both groups. On the other hand, although the IAM data calculated by Manero *et al* [22] also agree well with our data in shape, quantitatively, they overestimate systematically the DCS in the $10°$–$135°$ angular range.

In figure 3(a) we compare our experimental ICS in the 20–500 eV range with the calculated ICS of Morgan *et al* [21] at incident energies up to 50 eV and with the IAM data of Manero *et al* [22] in the 100–500 eV energy range. In general, our ICS are in good agreement with the theoretical results of Morgan *et al*. Surprisingly, despite the discrepancy seen between our experimental DCS and the IAM DCS of Manero *et al* [22] at 100 and 200 eV (see figure 2), there is a very good agreement in the ICS values in the energy range where the comparison is made. In order to understand this controversy, the interpolated–extrapolated data from our measured DCS at 100 and 200 eV are also shown in figure 2. It is seen that only at scattering angles less than $10°$ our extrapolated DCS is larger than the IAM results. Because CHF_3 is a strongly polar target (1.651 D) [8], it is quite reasonable to expect an enhancement of DCS near the forward direction. Nevertheless, the IAM calculation does not take this fact into account. It is also known that in the 100–500 eV energy range, the main contribution to the ICS comes from the DCS at small scattering angles ($\theta \leqslant 30°$). So, maybe a kind of error compensation between the contributions from small-angle and large-angle DCS to the ICS has taken place and resulting in the good agreement seen in ICS. In figure 3(b) we present our experimental MTCS in the 20–500 eV range along with the calculated MTCS of Morgan
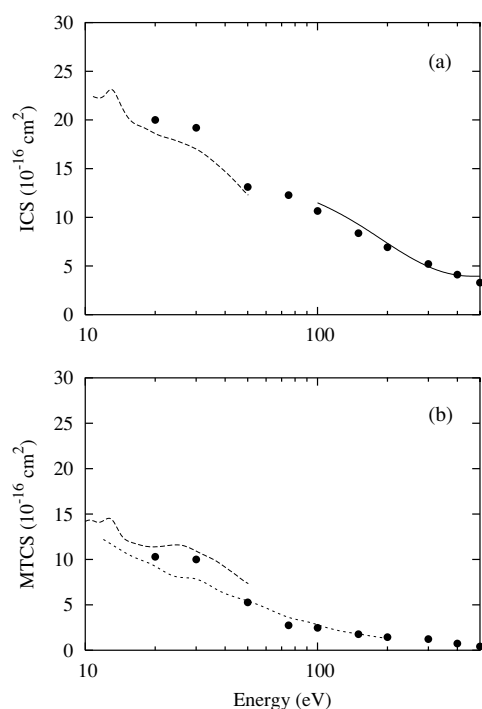
Figure 3. (a) ICS and (b) MTCS for e⁻–CHF₃ scattering. Full circles, present results; solid line, the IAM data of Manero *et al* [22]; dashed line, the calculated results of Morgan *et al* [21]; dotted line, the MTCS results of Kushner and Zhang [9].
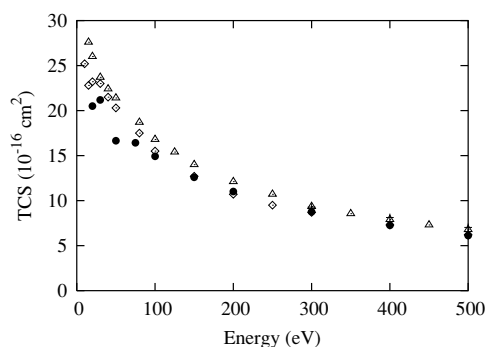

Figure 4. TCS for e⁻–CHF₃ scattering. Full circles, present estimated TCS; open diamonds, experimental TCS of Sueoka *et al* [10]; open triangles, experimental TCS of Nishimura and Nakamura [12]; pluses, experimental TCS of Iga *et al* [13].

et al [21] at incident energies up to 50 eV and the MTCS generated by Kushner and Zhang [9] in the 10–200 eV energy range. In the 20–50 eV, our MTCS lie between those of Morgan *et al* and of Kushner and Zhang. At higher energies, our data agree very well with those generated from swarm parameters [9]. In addition, we also made an estimate of the TCS by adding the experimental TICS of Iga *et al* [17] to our ICS. The estimated TCS are shown in figure 4, along with some experimental TCS available in the literature [10, 12, 13]. A general

good agreement between our estimated data and the existing experimental results [10, 12, 13] at incident energies above 100 eV is encouraging. As observed by Joshipura *et al* [33], the ionization channel dominates the inelastic processes, the TICS corresponding to about 80% of the total inelastic cross section at energies around 100 eV and going to near 100% for energies above 300 eV. At energies below 100 eV, our estimated TCS is about 10% lower than the experimental values of Sueoka *et al* [10] and about 30% lower than the experimental data of Nishimura and Nakamura [12], this difference may be attributed to the electronic excitation processes.

Acknowledgments

References

[1] Yanev V, Krischok S, Opitz A, Wurmus H, Schaefer J A, Schwesinger N and Ahmed S I U 2004 *Surf. Sci.* **566** 1229
[2] Goto M, Nakamura K, Toyoda H and Sugai H 1994 *Japan. J. Appl. Phys.* **33** 3602
[3] Jane R K 1993 *Atomic and Plasma-Material Interaction Processes in Controlled Thermonuclear Fusion* ed R K Janev and H W Drawin (Amsterdam: Elsevier) p 27
[4] Morgan W L 2000 *Adv. At. Mol. Opt. Phys.* **43** 79
[5] Christophorou L G, Olthoff J K and Rao M V V S 1997 *J. Phys. Chem. Ref. Data* **26** 1
[6] Christophorou L G and Olthoff J K 1999 *J. Phys. Chem. Ref. Data* **28** 967
[7] Tanaka H, Masai T, Kimura M, Nishimura T and Itikawa Y 1997 *Phys. Rev.* A **56** R3338
[8] Varella M, Winstead C, McKoy V, Kitajima M and Tanaka H 2002 *Phys. Rev.* A **65** 022702
[9] Kushner M J and Zhang D 2000 *J. Appl. Phys.* **88** 3231
[10] Sueoka O, Takaki H, Hamada A, Sato H and Kimura M 1998 *Chem. Phys. Lett.* **288** 124
[11] Sanabia J E, Cooper G D, Tossel J A and Moore J H 1998 *J. Chem. Phys.* **108** 389
[12] Nishimura H and Nakamura Y 2005 *J. Phys. Soc. Jpn.* **288** 124
[13] Iga I, Pinto P R and Homem M G P 1999 *Int. Symp. on Electron–Molecule Collisions and Swarms* unpublished
[14] Fiegele T, Hanel G, Torres I, Lezius M and Märk T D 2000 *J. Phys. B: At. Mol. Opt. Phys.* **33** 4263
[15] Poll H U and Meischner J 1987 *Contrib. Plasma Phys.* **27** 359
[16] Jiao C Q, Nagpal R and Haaland P D 1997 *Chem. Phys. Lett.* **269** 117
[17] Iga I, Sanches I P, Srivastava S K and Mangan M 2001 *Int. J. Mass Spectrom.* **208** 159
[18] Torres I, Martínez R and Castaño F 2002 *J. Phys. B: At. Mol. Opt. Phys.* **35** 2423
[19] Furuya K, Matsuo K, Koto E, Maruyama K, Hatano Y and Ogawa T 2002 *J. Phys. B: At. Mol. Opt. Phys.* **35** 1015
[20] Natalense A P P, Bettega M H F, Ferreira L G and Lima M A P 1999 *Phys. Rev.* A **59** 879
[21] Morgan W L, Winstead C and McKoy V 2001 *J. Appl. Phys.* **90** 2009
[22] Manero F, Blanco F and García G 2002 *Phys. Rev.* A **66** 032713
[23] Srivastava S K, Chutjian A and Trajmar S 1975 *J. Chem. Phys.* **63** 2659
[24] Khakoo M A and Trajmar S 1986 *Phys. Rev.* A **34** 138
[25] Tanaka H, Ishikawa T, Masai T, Sagara T, Boesten L, Takekawa M, Itikawa Y and Kimura M 1998 *Phys. Rev.* A **57** 1798
[26] Iga I, Lee M T, Homem M G P, Machado L E and Brescansin L M 2000 *Phys. Rev.* A **61** 227081
[27] Rawat P, Iga I, Lee M T, Brescansin L M, Machado L E and Homem M G P 2003 *Phys. Rev.* A **68** 052711
[28] Olander D R and Kruger V 1970 *J. Appl. Phys.* **41** 2769
[29] Register D F, Trajmar S and Srivastava S K 1980 *Phys. Rev.* A **21** 1134
[30] Buckman S J, Gulley R J, Moghbelalhossein M and Bennett S J 1993 *Meas. Sci. Technol.* **4** 1143
[31] Jansen R H J, de Heer F J, Luyken H J, van Wingerden B and Laauw H J B 1976 *J. Phys. B: At. Mol. Phys.* **9** 185
[32] Panajotović R, Filipović D, Marinković B, Pejčev V, Kurepa M and Vušković L 1997 *J. Phys. B: At. Mol. Opt. Phys.* **30** 5877
[33] Joshipura K N, Vinodkumar M and Patel P M 2000 *J. Phys. B: At. Mol. Opt. Phys.* **34** 509